Available online at www.sciencedirect.com
SCIENCE DIRECT®
Deep-Sea Research I 51 (2004) 979–997
DEEP-SEA RESEARCH PART I
www.elsevier.com/locate/dsr

Observed sediment fluxes in the southwesternmost Okinawa Trough enhanced by episodic events: flood runoff from Taiwan rivers and large earthquakes

Shih-Chieh Hsu[a,*], Fei-Jan Lin[b], Woei-Lih Jeng[b], Yu-chia Chung[c], Lih-Ming Shaw[b], Kuo-Wei Hung[c]

[a] *Institute of Earth Sciences, Academia Sinica, Taipei, Taiwan, ROC*
[b] *Institute of Oceanography, National Taiwan University, Taipei, Taiwan, ROC*
[c] *Institute of Marine Geology and Chemistry, National Sun Yat-sen University, Kaohsiung, Taiwan, ROC*

Received 18 December 2002; received in revised form 10 October 2003; accepted 20 January 2004

Abstract

The sediment fluxes to the southwesternmost Okinawa Trough (SOT) off northeast Taiwan have been measured with four sets of sediment traps. The sediment fluxes observed were much higher than those in many marginal seas and showed great variations in time and space. The fluxes exhibited a drastic seaward decline from northeastern Taiwan to the central trough and an increase with depth. Temporal variability of fluxes was in a wide range from three times to one order of magnitude for certain traps. The observed sediment fluxes had a positive correlation with river runoff from the Lanyang Hsi, a river in northeastern Taiwan. Usually, the highest fluxes could be attributed to episodic events, for example, typhoon passages, which always cause ample rainfall leading to high runoff and sediment discharge, and sediment fluxes that were observed during typhoon passages accounted for more than 50% of the long-term flux. Large earthquakes are suggested to be responsible for some sediment flux anomalies observed on the nearby steep slope because of a good match in time between sediment collection and earthquake occurrence. A conceptual model is proposed to illustrate the sources and transport of the SOT sediment. The study highlights the greater contribution of Taiwan fluvial sediments to the SOT compared to that of the Changjiang, and it provides evidence demonstrating the combined effects of river runoff and large earthquakes on the sediment fluxes observed in such a deep marginal sea.

Keywords: Sediment flux; River runoff; Earthquake; Episodic event; Okinawa Trough; Taiwan

1. Introduction

Apart from source strengths, a variety of factors have been considered to be regulating the sediment fluxes in the seas, such as primary production (Nair et al., 1989), scales and directions of oceanic

*Corresponding author. Tel.: +886-2-27839910x252; fax: +886-2-27833584.
E-mail address: schsu@earth.sinica.edu.tw (S.-C. Hsu).

0967-0637/$ - see front matter © 2004 Elsevier Ltd. All rights reserved.
doi:10.1016/j.dsr.2004.01.009

flows (Honjo et al., 1980), monsoons inducing changes of oceanic circulation patterns (Nair et al., 1989), and river discharge directly from land (Ittekkot et al., 1991; Wheatcroft, 2000). Recently, a comprehensive investigation, the STRATAFORM program, was undertaken to evaluate the supplies of storm driven river sediment to the northern California shelf (Nittrouer, 1999; Wheatcroft, 2000). Researchers have documented that such episodic small-river floods could account for much of the annual sediment flux to the continental shelf and slope. Large earthquakes are able to induce instabilities and then sliding/slumping of slope sediments in the tectonically active continental margins (Hasiotis et al., 2002; Lykousis et al., 2002). Owing to the natural forces mentioned above, medium- to large-scale submarine mass movements can occur and thus play a very important role in transport of terrigenous sediment to deep basins (Mulder and Cochonat, 1996).

Data on sediment fluxes obtained from four sets of sediment traps deployed in the southwesternmost Okinawa Trough (SOT), as well as data on particulate Al (PAl) in total suspended matter (TSM) along four transects (one each along shelf, slope and trough and one across shelf trough) were acquired in this study. Al was used as an indicator of the lithogenic (aluminosilicate) component of TSM and settling sediments (trap samples) (Hsu et al., 1998). During the collection period, there were several typhoons sweeping over northern Taiwan and large earthquakes ($M \geqslant 5.0$ R) occurring with epicenters located beneath the study area. The study aimed to (1) determine the temporal and spatial variations in the sediment flux, (2) examine the source and transport mechanisms of the sediments, and (3) evaluate the significance of episodic events (i.e. flood runoff and large earthquakes) as they might be reflected in observed flux extremes.

2. Geological setting and circulation patterns

Tectonically, the Okinawa Trough, situated between the East China Sea (ECS) shelf and the Ryukyu Islands (inset to Fig. 1), is an active back-arc basin. The SOT borders northeastern Taiwan and is the deepest and narrowest part of the Okinawa Trough. Large earthquakes frequently occur in the region, where the Philippine Sea plate collides with and then subducts beneath the Eurasian plate. Usually, earthquake epicenters are located beneath the land area of eastern Taiwan and the seafloor off eastern Taiwan. In the SOT, sediments are approximately 1–3 km thick (Lee et al., 1980; Letouzey and Kimura, 1986; Sibuet et al., 1987). Sedimentation rates are from 0.18 to 0.87 cm/yr in a small quadrangle (ca. 2000 km^2) in the SOT (Fig. 1) off northeastern Taiwan, and dramatically decrease to less than 0.1 cm/yr outside this quadrangle (Chen, 1995; Chung and Chang, 1995). Also, the preliminary results from site 1202 (24°48.24′N, 122°30.00′E, 1275 m) of ODP Leg 195 in the SOT showed a very high-sedimentation rate of at least 325 cm/kyr (0.325 cm/yr) (http://www-odp.tamu.edu/publications/pubs.htm), comparable to the above values. This rate may be the largest ever found in seas with depths of the SOT or deeper.

The Changjiang annually delivers 478 Mt of sediment onto the ECS shelf (Milliman and Meade, 1983), of which a substantial fraction (ca. 60%) is transported southward along the mainland China coast by the Changjiang Coastal

Fig. 1. (a) Regional map of circulation patterns over the ECS and the Okinawa Trough. There are three main currents occurring in this large-scale region: the Kuroshio, the TWC and the CCC. The Kuroshio collides with the shoaling ECS shelf off northeastern Taiwan; as a consequence, a portion of the Kuroshio intrudes upon the ECS shelf and thus forms a branch called the Kuroshio Branch (KB, shown in Fig. 1b). At the same time, a cyclonic eddy (CE) develops around the shelf break, shown in Fig. 1b. In addition, another current that may be involved in the flow systems and influence the transport and sedimentation of terrigenous sediments is the Yellow Sea Coastal Current (YSCC). (b) Sites of four sets of sediment trap mooring array deployments in the SOT and four transects (22 sites) along shelf, slope and trough and crossing the shelf–slope–trough for TSM sampling. The plaided quadrangle indicates a high-sedimentation area (> 0.2 cm/yr). Earthquake data were recorded at the Toucheng observation station of the Central Weather Bureau, Taiwan, ROC.

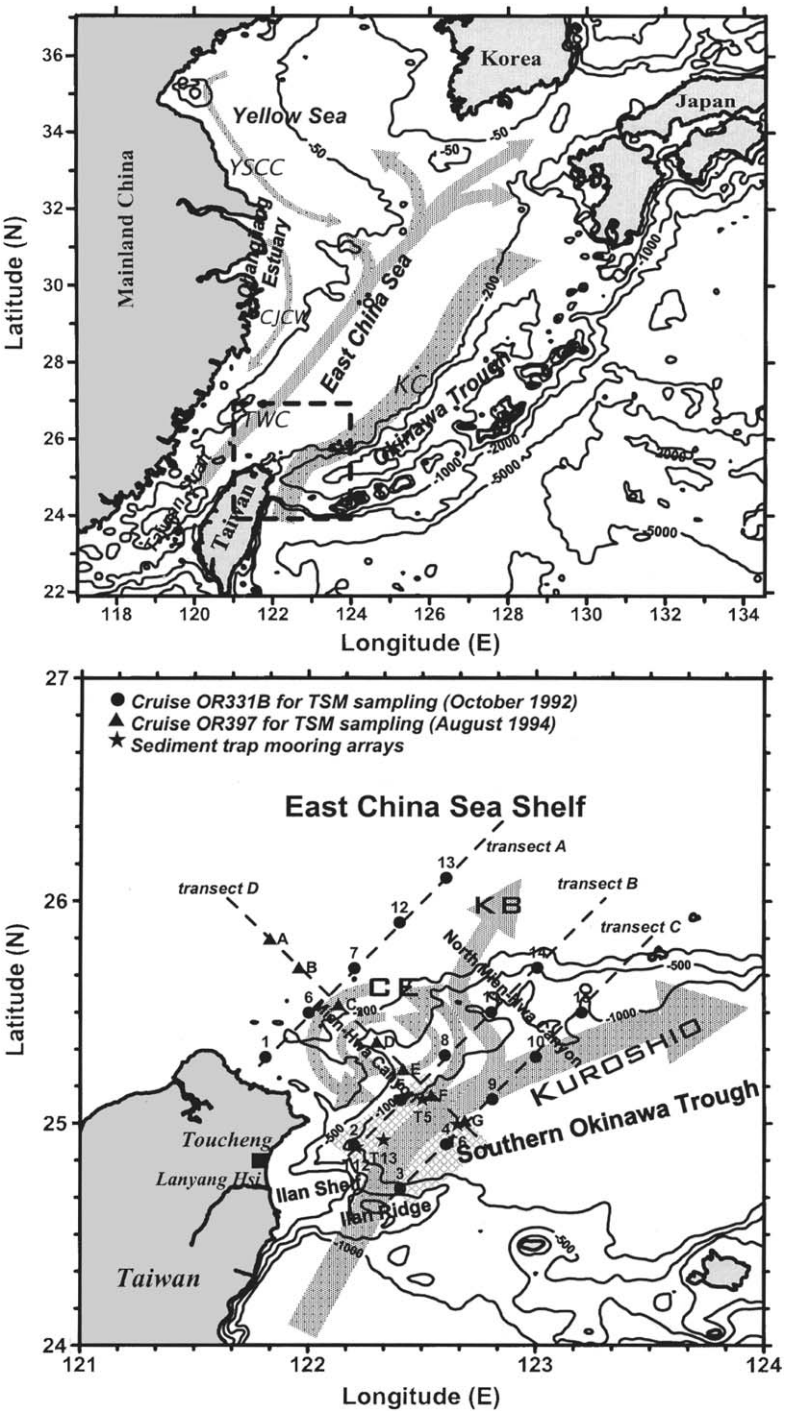
Korea
Japan
Yellow Sea
YSCC
Mainland China
Qiantangjiang Estuary
CJCW
East China Sea
KC
TWC
Okinawa Trough
Taiwan Strait
Taiwan
Latitude (N)
Longitude (E)
Cruise OR331B for TSM sampling (October 1992)
Cruise OR397 for TSM sampling (August 1994)
Sediment trap mooring arrays
East China Sea Shelf
transect A
transect B
transect C
transect D
KB
CE
North Mianhua Canyon
Tai-Hua Canyon
KUROSHIO
Southern Okinawa Trough
Toucheng
Lanyang Hsi
Ilan Shelf
Ilan Ridge
Taiwan

Current (CCC) (Fig. 1a) or tidal currents (Milliman et al., 1985). The wide ECS outer shelf, however, is covered by abundant relict sediments on the seafloor; they are composed mainly of biogenic debris, shell fragments and light brown sand remaining from the last glaciation (Boggs et al., 1979); no apparent sedimentation of contemporary sediments was observed on the outer shelf (Chen et al., 1992). Additionally, because of the high denudation rate (Li, 1976) and ample rainfall, Taiwan's rivers annually deliver an enormous 263 Mt of sediment to the sea (191 Mt from western Taiwan and 72 Mt from eastern Taiwan) (Milliman, 1991; Water Resources Planning Commission, 1996; Water Resources Bureau, 1997a, b), a portion of which could be carried northward by currents (i.e. the Kuroshio off eastern Taiwan and the Taiwan Warm Current (TWC) in Taiwan Strait, see Fig. 1a) toward the study area. The large supply of terrestrial sediments from Taiwan and China thus appears to be sufficient to account for the accumulation in the high-sedimentation-rate part of the SOT (Fig. 1b), which is less than 10 Mt/yr (Hsu, 1998). Nevertheless, the source of the SOT sediment has been debated for over two decades. Earlier efforts to identify the sources (e.g. the Changjiang or Taiwan's rivers) and transport pathways of the SOT sediment were based on diverse tools, e.g. chemical characteristics, mineralogy and physical properties of the sediments (Lin and Chen, 1983; Chen et al., 1992; Li, 1994; Chung and Chang, 1995, 1996). On the basis of the spatial distribution of PAl concentrations, hydrographic properties (such as temperature and salinity) as well as circulation patterns, Hsu et al. (1998) concluded that terrigenous sediment from eastern Taiwan rivers is probably the main source.

This study further explored the positive relationship between the observed sediment fluxes in the SOT and runoff of the Lanyang Hsi, a river in northeastern Taiwan. The annual sediment discharge and sediment yield of the Lanyang Hsi are 8.0 Mt and 8154 Mt/km^2, respectively. The annual runoff is 2773×10^6 m^3 and transient runoff always rises sharply from a baseline level of several tens of m^3/s (mean rate 62 m^3/s) to an abnormal level of thousands of m^3/s after heavy rainfall (average annual rainfall 3256 mm). The historical maxima of the daily runoff and of suspension concentration are 4580 m^3/s and 118 g/l, respectively, since 1949 (Water Resources Bureau, 1997a, b). The sediment discharges are dependent on river runoff, and a function relating the two has been established (Kao, 1995).

The main flow affecting this study area is the Kuroshio, which flows northward along the eastern coast of Taiwan (Fig. 1). As it approaches northeastern Taiwan, it impinges on the shoaling ECS shelf; thereafter the Kuroshio mainstream turns northeastward almost along the shelf break. Part of the Kuroshio water intrudes onto the shelf forming a branch current, called the Kuroshio Branch Current. On the western side of the branch current, a cyclonic eddy about 70 km in diameter is generated over the shelf–slope as a result of the westward deflection of part of the branch current. According to Hsu et al. (1998), the Kuroshio may bring abundant fluvial sediments exported from eastern Taiwan rivers, in particular the Lanyang Hsi, to the SOT. The TSM in the upper water can be entrained into the cyclonic eddy and accumulate around the eddy's center. Hence, for the shallower water the cyclonic eddy may play an important role in transporting surface suspensions seaward.

There are two other major current systems involved in the circulation of the ECS (Fig. 1a). One, the previously mentioned CCC flows southward along the mainland China coastline, and the other, the TWC flows northward along Taiwan Strait and is expected to bring fluvial sediments exported from western Taiwan rivers. It has been demonstrated that the TWC prevents the southward-transported Changjiang sediments from spreading to the outer shelf and thus confines these sediments to the inner shelf (Milliman, 1991; Su, 2000).

3. Materials and methods

Sediment fluxes were obtained at four moorings (T5, T6, T12 and T13) with sediment traps at two or three depths per mooring in the SOT (Table 1,

Table 1
Basic parameters for sediment traps deployed off northeastern Taiwan

Station ID	Latitude (N)	Longitude (E)	Bottom depth (m)	Cup depth (m)	Current meter depth (m)	Deployment period	Collection duration (days/cup)
T5	25°06.45′	122°30.06′	1060	560 (12)[a], 760 (12), 960 (12)	365, 565, 765	5/5/1994–9/1/1994	10
T6	24°59.63′	122°39.26′	1440	740 (12), 1340 (12)	896, 1196	11/14/1994–5/12/1995	15
T12	24°53.37′	122°12.38′	1017	569 (15), 768 (16), 967 (12)	581, 780, 972	3/23/1996–8/19/1996, 10/7/1996–1/4/1997	15
T13	24°55.36′	122°19.57′	1392	946 (16), 1144 (16), 1343 (16)	951, 1244	3/23/1996–8/19/1996, 10/7/1996–1/4/1997	15

[a] ( ) = sample numbers.

Fig. 1b). French-made time-series PPS3 sediment traps (Piege a Particules Sequentiel, Model 3) were used (Heussner et al., 1990), which comprise 12 receiving cups and have a receiving area of 0.125 m^2. Current meters were attached between traps. Sample treatment procedures are described elsewhere (Chung and Hung, 2000). The Al abundance in samples from T5 and T6 was measured; samples from T12 and T13 arrays were not analyzed because they were expected to be similar to those from T5 and T6, which were dominated by lithogenic sediments, as described below.

The TSM samples for analyzing Al were collected on cruises OR331B (10/4–9/1992) and OR397 (8/10–17/1994) of R./V. *Ocean Researcher I* of National Taiwan University (Fig. 1b). Cruise OR397 comprised three NE–SW parallel transects, along the shelf (transect A), slope (transect B) and trough (transect C), and each transect contained five stations. Cruise OR331B sampled seven stations in one NW–SE transect (transect D), crossing the ECS shelf to the trough and perpendicular to transects A, B and C. Cruise OR397 was taken 3 days after the landfall of typhoon Doug on northern Taiwan, and was in the collection period of trap T5. TSM samples were obtained through a filtration of 20–60 l seawater. Seawater samples were collected from varying depths with a CTD rosette equipped with twelve 20-l precleaned GO-FLO bottles.

Al and Fe determinations were made with a Hitachi 8100 flameless atomic absorption spectrophotometer (graphite furnace) after total digestion. Compositional data quality was validated by determinations of standard reference material BCSS-1 (marine sediment). The details of sampling and analysis are given in Hsu et al. (1998, 2003).

4. Results and discussion

4.1. Spatial and temporal variations of the observed sediment fluxes

Temporal variations of the observed sediment fluxes for four sets of trap arrays are displayed against cup sequences in the lower panels of Figs. 2–5. Ranges and means of the sediment flux (Table 2) were 1.7–43 and 8.8 $g/m^2/d$ for array T5 ($n = 36$), 1.3–7.5 and 4.0 $g/m^2/d$ for array T6 ($n = 24$), 4–95 and 46 $g/m^2/d$ for array T12 ($n = 43$) and 6.1–36 and 17 $g/m^2/d$ for array T13 ($n = 48$), respectively. They show large spatial and temporal variability, and are much larger than those of the Middle Okinawa Trough (Narita et al., 1990) and many marginal seas (Gardner, 1989; Monaco et al., 1990; Biscaye and Anderson, 1994; Heussner et al., 1999). The time-series patterns of sediment flux showed: (1) a strong time-dependence, for example, the T5 fluxes varying over one

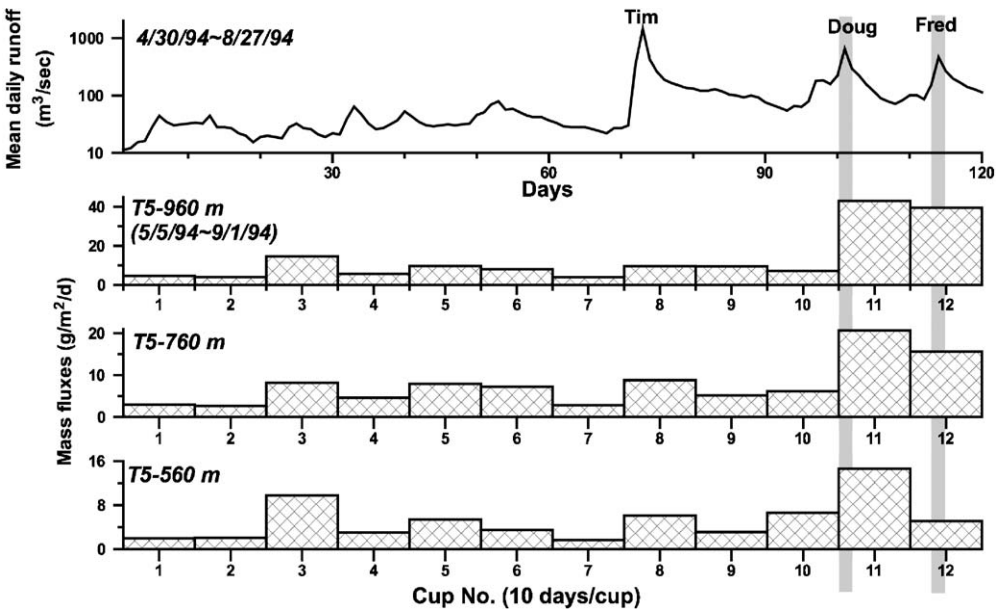

Fig. 2. Time-series of the Lanyang Hsi mean daily runoff (m^3/s) (upper panel) and the observed fluxes ($g/m^2/d$) at three depths from the T5 array (lower three panels). In the former, time was shifted back 5 days (from 4/30 to 8/27/1994) relative to the observation period of the T5 fluxes (from 5/5 to 9/1/1994). Three typhoons struck Taiwan during the T5 collection period; the runoff peaks caused by them may correspond to high fluxes, indicated by gray bars. Two flux maxima (cups 11 and 12) were evidently responsive to runoff peaks occurring during passage of typhoons Doug (8/6–8/8/1994) and Fred (8/18–8/21/1994). On the other hand, the extraordinary high runoff resulting from typhoon Tim's passage (7/10/1994) did not enhance the flux recorded in cup 8. Note that a logarithmic scale is used for the mean daily runoff.

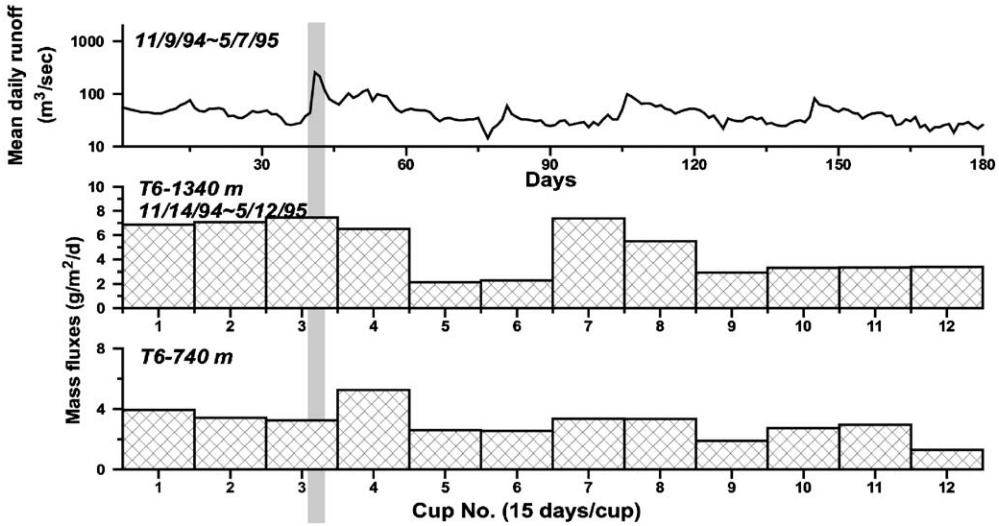

Fig. 3. As in Fig. 2, but for the T6 fluxes. Time-series of the Lanyang Hsi mean daily runoff was shifted back 5 days (from 11/9/1994 to 5/7/1995) relative to the observation period of the T6 fluxes (from 11/14/1994 to 5/12/1995). No typhoon took place during the T6 collection period. One runoff peak may correspond to the flux maximum observed in cup 3 of the 1340 m trap, but not to that of the 740 m trap, as indicated by the gray bar.

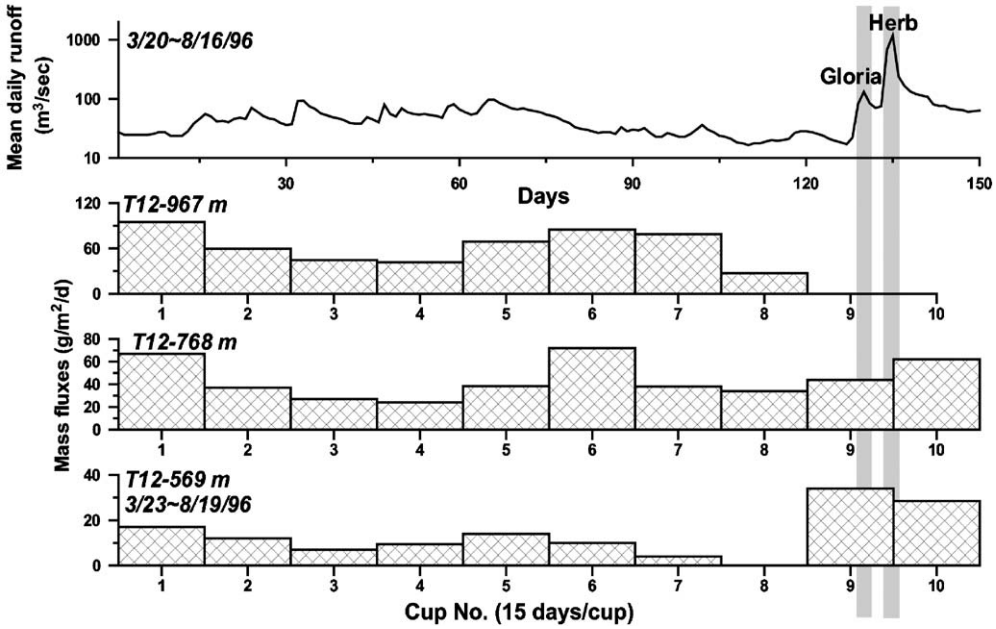

Fig. 4. As in Fig. 2, but for the T12 fluxes. Time-series of the Lanyang Hsi mean daily runoff was shifted back 3 days (from 3/20 to 8/16/1996) relative to the observation period of the T12 fluxes (from 3/23 to 8/19/1996). Typhoons Gloria (7/25–7/27/1996) and Herb (7/29–8/1/1996) occurred during the T12 collection period.

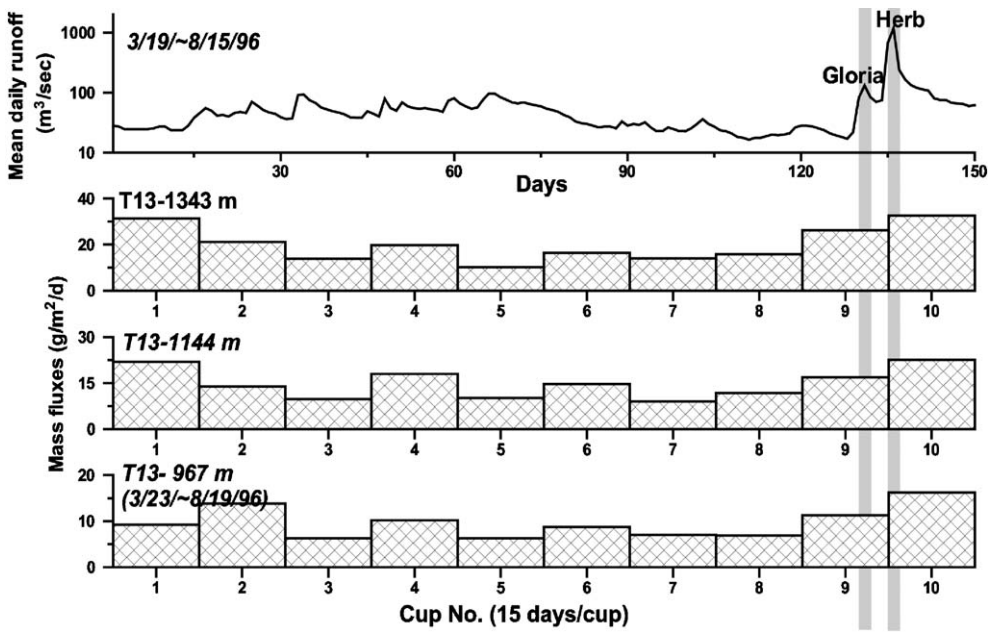

Fig. 5. As in Fig. 4, but for the T13 fluxes. Time-series of the Lanyang Hsi mean daily runoff was shifted back 4 days (from 3/19 to 8/15/1996) relative to the observation period of the T13 fluxes (from 3/23 to 8/19/1996).

Table 2
Sediment fluxes ($g/m^2/d$) measured for four sets of sediment traps deployed in the southwestern Okinawa Trough off northeastern Taiwan

Cup no.	T5			T6		T12			T13		
	560 m	760 m	960 m	740 m	1340 m	569 m	768 m	967 m	946 m	1144 m	1343 m
1	2.0	3.0	4.7	3.9	6.9	16.9	67.9	94.8	9.4	31.6	21.8
2	2.1	2.7	4.1	3.4	7.1	12.2	36.4	59.5	14.0	21.3	14.4
3	9.8	8.2	14.7	3.2	7.5	6.9	26.4	44.1	6.1	14.2	9.2
4	3.0	4.6	5.7	5.3	6.5	9.7	23.4	41.4	10.2	20.0	18.1
5	5.4	7.9	9.8	2.6	2.2	13.7	38.2	69.2	6.1	10.2	9.9
6	3.5	7.3	8.0	2.6	2.3	9.9	71.9	84.6	8.5	16.6	14.7
7	1.7	2.8	4.0	3.3	7.4	4.0	37.2	78.8	6.9	14.3	8.9
8	6.1	8.8	9.7	3.3	5.5	—	32.5	26.3	6.7	15.8	11.6
9	3.1	5.1	9.5	1.9	2.9	33.4	44.0	—	11.4	26.2	17.1
10	6.6	6.1	7.2	2.7	3.3	27.6	72.6	—	16.4	32.6	22.8
11	14.6	20.7	42.9	3.0	3.3	12.1	64.4	72.2	13.5	24.4	20.3
12	5.1	15.6	39.5	1.3	3.4	21.8	71.0	80.1	13.5	22.8	21.0
13						30.4	78.1	78.1	16.7	35.7	23.9
14						39.2	89.4	36.7	15.0	30.8	27.4
15						27.8	87.4	—	12.7	32.1	23.6
16						31.6	79.5	—	9.4	20.5	17.3
Mean [a]	5.3	7.7	13.3	3.0	4.9	19.8	57.7	63.8	11.0	23.1	17.6
Mean [b]		8.8		4.0			46.2			17.2	

— Sampling failures.
[a] Mean values of various depth trap fluxes.
[b] Mean values of each set of trap fluxes.

order of magnitude, (2) synchronized variations between various depths for each set of trap arrays, and (3) constant (less variable) but low fluxes for T6 relative to others. These three features reveal three facts. First, many flux extremes (e.g. cups 11 and 12 of T5) could probably be attributed to certain episodic events (e.g. heavy rain during typhoon passages) that enhance quantities and rates of sediment supply, which will be discussed below. Second, the sources of settling sediments were almost similar at least for individual trap arrays, but the source strength was temporally changeable. Third, constant but low fluxes for T6 indicate that there were persistent and stable sources of sediment laterally contributing to the central SOT sediments.

The vertical profiles of mean fluxes at certain depths for each set of trap arrays are shown in Fig. 6a; horizontal trends of mean fluxes for each set of trap arrays are shown against relative distances to station T12 (Fig. 6b). The spatial patterns of observed fluxes were characterized by two major features. First, the fluxes increase with increasing depth (except for T13); this was usually found in marginal seas (Honjo et al., 1980, 1982; Saito et al., 1992; Biscaye and Anderson, 1994), illustrating that the transport of SOT sediments depended upon lateral advection in mid-depth water and bottom transport in deep water. Second, the fluxes largely decrease offshore from the northern slope of the Ilan Shelf and Ridge (T12 and T13) to the outlet of the Mien-hwa Canyon (T5) and the central trough (T6). Generally, the decreasing trends of fluxes are consistent with those of the PAl distribution (Hsu et al., 1998), as will be discussed in Section 4.3. Furthermore, the abnormally high fluxes observed on the lower slope north to the Ilan Shelf and Ridge demonstrated that the depositing environment is very dynamic, which will always cause sediment redistribution

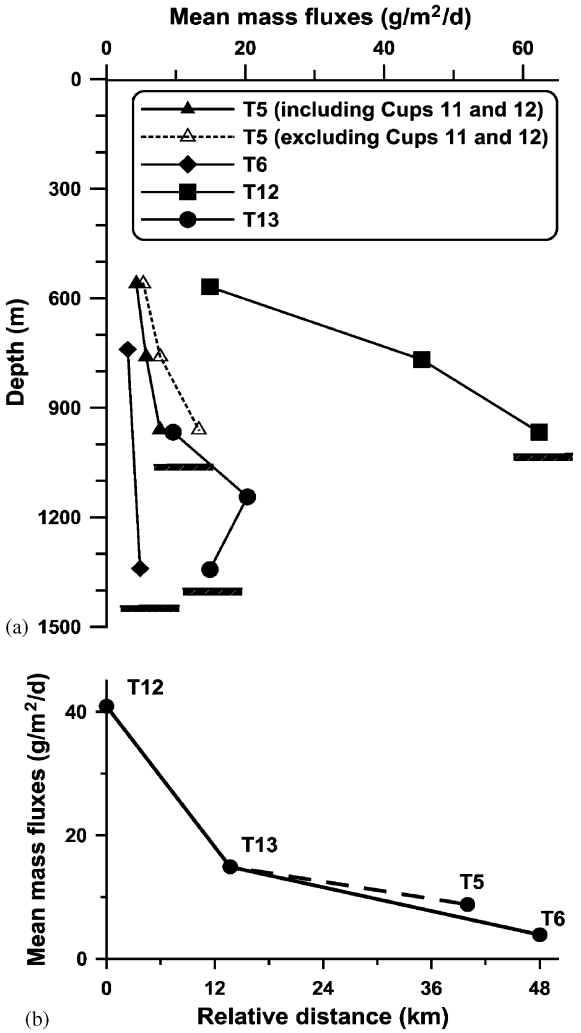

Fig. 6. (a) Vertical distribution of mean fluxes (g/m^2/d) at certain depths for four sets of sediment trap mooring arrays. (b) Horizontal distribution of mean fluxes for each trap array relative to station T12.

and then contribute sufficient sediments to the SOT (Chen et al., 1992; Hsu et al., 1998; Lee, 2001).

4.2. Components and chemical compositions of settling sediments

Al abundance of the settling sediments from both T5 and T6 trap arrays averages 7.8% and 8.8%, respectively; Fe abundance, 3.9% for T5 samples and 4.1% for T6 samples (Table 3). This is in agreement with those determined for the SOT surface sediments, Al and Fe abundances being $8.2\pm1.3\%$ and $4.4\pm0.7\%$, respectively (Hsu et al., 2003). Given that the Al abundance of lithogenic particles is similar to that of the average crust composition (8%) (Taylor, 1964), it allowed us to estimate the fraction of lithogenic components accounting for the bulk sediment (at least 80% or more). Such an estimate is reasonable because the total organic carbon (TOC) and carbonate of T6 trap samples account for a minor fraction, less than 2% and less than l0%, respectively (Sheu et al., 1999). This also agrees with the result of grain size analysis which shows that both T5 and T6 samples are dominated by silt and clay (more than 90% for most samples) (Chung and Hung, 2000). No obvious trends were found to illustrate the seasonal variations in TOC (or total organic matter, TOM) related to the primary production in the euphotic zone and those in grain size related to hydrodynamics (Sheu et al., 1999; Chung and Hung, 2000). In addition, based on the study of Chen et al. (1992), the mean grain size of the SOT surface sediment is quite fine and uniform, i.e. 7–8ϕ; the clay fraction accounts for $\sim$50% of the

Table 3
Ranges and means ($\pm$1 s.d.) of Al and Fe abundances (wt%) for T5 and T6 trap samples

	Depth (m) (sample no.)	Al (%)		Fe (%)	
		Range	Mean $\pm$ 1 s.d.	Range	Mean $\pm$ 1 s.d.
T5	560 ($n=9$)	6.8–9.1	7.7 ± 0.7	3.4–4.3	3.8 ± 0.3
	760 ($n=12$)	7.1–8.8	7.9 ± 0.6	3.7–4.2	3.9 ± 0.2
	960 ($n=9$)	7.2–8.4	7.8 ± 0.5	3.6–4.2	4.0 ± 0.2
T6	740 ($n=12$)	7.9–9.1	8.8 ± 0.4	3.9–4.1	4.0 ± 0.1
	1340 ($n=12$)	8.4–9.4	8.7 ± 0.3	4.0–4.3	4.1 ± 0.1

bulk sediment; the carbonate consists of ~10% of the bulk sediment. They concluded that the terrigenous sediment is the most predominant component of the SOT sediment, consistent with results of the trapped sediment in this work and of the surface sediment (Hsu et al., 2003). Accordingly, high terrigenous fractions may mask the signatures of low biogenic fractions (Sheu et al., 1999), thus resulting in insignificant seasonal patterns of the biogenic fluxes observed.

4.3. Nepheloid layers elucidated by the PAl spatial distribution

For cruise OR331B, PAl concentrations range from 0.4 to 36.7 μg/l with a mean of 4.4 ± 7.1 μg/l; for cruise OR397, PAl concentrations range from 0.2 to 135 μg/l with a mean of 7.0 ± 20.3 μg/l. The PAl depth profiles along four transects (A, B, C and D) investigated are displayed in Fig. 7, and have provided more insights into the spatial distribution of aluminosilicate (i.e. terrigenous) particles in the water column for tracing possible sources and depicting transport routes of the SOT sediment.

As shown in Fig. 7a, the PAl concentrations along transect A decrease seaward from the Taiwan coast (station 1) to offshore regions (station 13). They are low but uniform (approximately ⩽10 μg/l) throughout the water column at offshore stations (station 6 and farther stations). It reveals that the PAl in the shelf water has undergone thorough mixing, possibly driven by tidal currents or internal waves. It further indicates that terrigenous particles transported offshore were quickly deposited (Windom and Gross, 1989; Naudin et al., 1997) or that the particle-rich coastal water was diluted by the particle-poor Kuroshio water.

As shown in Fig. 7b, high PAl concentrations along transect B were found in the upper water levels, extending from the coast (e.g. station 2) to the center of a cyclonic eddy (station 8) located around the shelf break (Fig. 1b) (Hsu et al., 1998; Tang et al., 1999). This suggests that terrigenous particles were entrained into the eddy and then accumulated around its center (Hsu et al., 1998). Hsu et al. (1998) observed low temperature and low salinity in water occupying the coastal region (e.g. stations 2, 3, 4 and 5) and suggested large volumes of river discharge exported from eastern Taiwan (e.g. Langyang Hsi), particularly during or after typhoon passages. Meanwhile, rivers can be expected to export huge volumes of suspended sediments. PAl concentrations in the offshore water (stations 11 and 14) drastically decline throughout the water column, with a low PAl zone appearing at a depth of 200–500 m around the eddy center (station 8). Apparently, the PAl-poor water observed on transects A and B reflects the intruded "clean" Kuroshio water. By contrast, high PAl was found at ~600 m around the northern slope of the Ilan Shelf (e.g. stations 2 and 5) where the environment may be unstable primarily owing to steep topography (>3°) and tectonic settings as well as strong flows. Such a high PAl plume likely forms nepheloid layers (represented by shaded area in Fig. 7b), dispersing suspended sediments into the SOT.

As shown in Fig. 7c, the general patterns of the PAl profile along transect C were similar to those along transect B. There were elevated PAl concentrations near the coast and low PAl concentrations (less than 10 μg/l) off the coast. Two slightly higher PAl concentrations extending northeastward from the coastal zone (station 3) were found in the middle water layers. Additionally, a pronounced PAl concentration (135 μg/l) was found in near-bottom water layers on the slope (920 m at station 3) that most likely originated from the same source (or mechanism) as that observed at station 2, and it declined sharply toward the trough. The Al plume probably forms nepheloid layers. Note that the isopleth of 20 μg/l seems not to extend as far as station 15 (Fig. 7c) because sampling intervals were not close enough to verify the dispersing distance for the strong PAl plume. Nevertheless, it is believed that the plume can influence the PAl concentration to a large extent, at least up to the trough (e.g. station 10).

As shown in Fig. 7d, the PAl distribution was characterized by two main features along transect D: (1) PAl concentrations were generally lower in the shelf water than those in the slope and trough water, and (2) two PAl maximum zones were

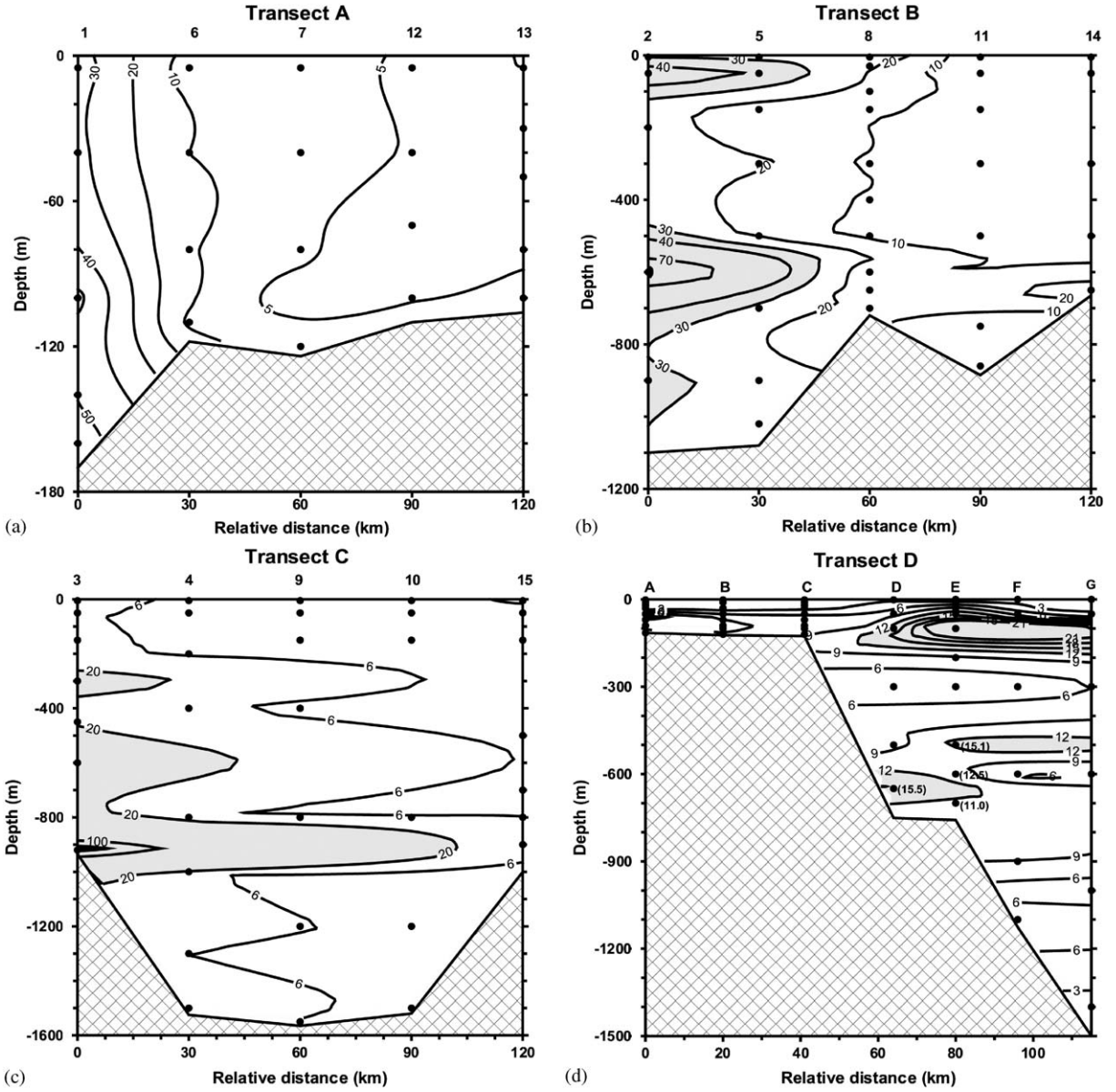

Fig. 7. Vertical distributions of the PAl concentrations (μg/l) on four transects (a) A (along the shelf), (b) B (along the slope), (c) C (along the trough) and (d) D (crossing the shelf–slope–trough). Several PAl plumes are represented by shaded areas, which may be nepheloid layers. Note that different contour intervals were used for individual plots.

found in the subsurface water (about 100 m) and at mid-depth (500–700 m) at slope–trough stations (stations D, E, F and G). Apparently, this high PAl subsurface zone did not result from cross-shelf transport of suspended particles from the ECS shelf (e.g. stations A, B and C) to the slope and trough. It revealed that high terrigenous particles in subsurface slope water would come

predominantly from eastern Taiwan (or the north slope of the Ilan Shelf and Ridge); this is consistent with results from stations 2 and 3 of cruise OR397. Moreover, the PAl mid-depth maximum could be caused by lateral transport of resuspended slope sediments (on the ECS slope or the north slope of Ilan Shelf and Ridge). However, it did not allow us to conclude if particle contributions from station D (ECS slope) were adequate for station E because gradients of PAl concentrations between 600 m at station D (15.5 μg/l) and 500–700 m at station E (11.0–15 μg/l) were insignificant. It is therefore suggested that there was another source from a different direction accounting for the high PAl layer. Downslope transport of redistributed sediments on the north slope of Ilan Shelf and Ridge, which were caused by disturbances such as resuspension, slumping or sliding and had a dispersal direction perpendicular to transect D, appeared to be the major source of sediments. Apparently, this source is identical to the middle and deep PAl (or suspended matter) plumes observed on transects B and C (Figs. 7b and c).

There were several PAl plumes found in the upper (~100 m), middle (~600 m) and deep (~900 m) waters (Fig. 7); in general, they extended from the coastal zone to the offshore region (or the trough). On the basis of hydrographic measurements, river-borne sediments delivered from the Lanyang Hsi were the most probable source responsible for the upper PAl plume (Hsu et al., 1998). In addition, sediments deposited on the northern slope of the Ilan Shelf and Ridge off northeastern Taiwan can be easily disturbed by diverse dynamic flows (including currents and tides) and tectonic movement (e.g. submarine earthquakes). Turbidites have been commonly found in the lower slope sediments in the southwestern Okinawa Trough (Chen et al., 1992), so they must frequently lead to mass movement of slope sediments. The reworked sediments thus were laterally advected toward the trough and enhanced the PAl content in the water. These plumes might become nepheloid layers that always serve as a critical transport mechanism (or source) for the basin sediment (Monaco et al., 1990; De Hass and Van Weering, 1997).

4.4. Sediment fluxes related to river runoff

A graph-matching method (comparing the time-series of sediment fluxes observed from each trap and of the mean daily runoff of the Lanyang Hsi undergoing shifts of 0–7 days) was used to examine the correlation of the above two parameters; results are shown in Figs. 2–5. Some peak data of daily runoff were identified to correlate with high fluxes. For example, typhoons Doug (8/6–8/8/1994) and Fred (8/18–8/21/1994) caused such high runoffs (652 and 468 m^3/s, respectively) that sediment fluxes peaked at cups 11 and 12 of array T5 (Fig. 2 and Table 2). Typhoon Herb (7/29–1/8/1996) also caused relatively high runoff (1180 m^3/s), which consequently caused a high sediment flux observed at cup 10 of both arrays T12 and T13 (Figs. 4 and 5). These facts revealed that once typhoons struck Taiwan, heavy rainfall always caused high runoff together with huge sediment export from the land, thus contributing to the source of settling sediments. Unfortunately, it appeared that not all flood events necessarily cause high fluxes. For example, typhoon Tim (7/9–7/11/1994) created very high runoff (up to 1440 m^3/s) and thus very high suspensions of about 10,000 mg/l (Kao, 1995), but it did not cause remarkable sediment flux as expected (Fig. 2). Even so, we cannot be sure if this resulted from sampling biases, because trapped sediments seemed to overstuff the receiving cup (T5-cup 8).

Furthermore, a relationship was examined between the sediment flux and the Lanyang Hsi river discharge. The total river discharge for certain periods, corresponding to the flux observed in a given cup, was the integration of the Lanyang Hsi mean daily runoff for the collection periods (shifted). For instance, the collection period of array T5-cup1 was from 5/5 to 5/14/1994, so the total river discharge corresponding to the T5-cup1 is the sum of the mean daily runoff for a period of 10 days, i.e. 4/30–5/9/1994, this period was shifted back 5 days (relative to 5/5–5/14/1994). As a consequence, we found a significant log–log positive correlation between the observed flux and the total runoff for almost all traps even though there are a few outliers from regression lines (Fig. 8). If there were any typhoon passing

through Taiwan during the collection period for certain cups, the data of these cups were labeled by a "*t*" in related plots. Moreover, the high fluxes due to flood events, particularly during typhoon passages, generally account for a major fraction of the long-term fluxes, particularly for the central trough; for example, cups 11 and 12 accounted for at least 52% of the total fluxes for half a year for array T5. In fact, the peak fluxes would have appeared in several days (very likely in less than 3 days) and would be much larger than observed values (i.e. averaging the whole collection period), so the significance of the flood events to the SOT sediment is inferred to be much greater than the above estimate. In addition, the log–log relationship between the flux and river runoff reflects two facts: (1) there is an exponential relationship between the riverine particle concentration and river discharge, as discussed by Kao (1995), and (2) concentrations of the suspended particulate plumes that developed after tremendous fluvial sediments were exported from the Lanyang Hsi river mouth declined exponentially with dispersing distances (this is in agreement with sediment transport models) (Lyne et al., 1990; Zhang et al., 1999).

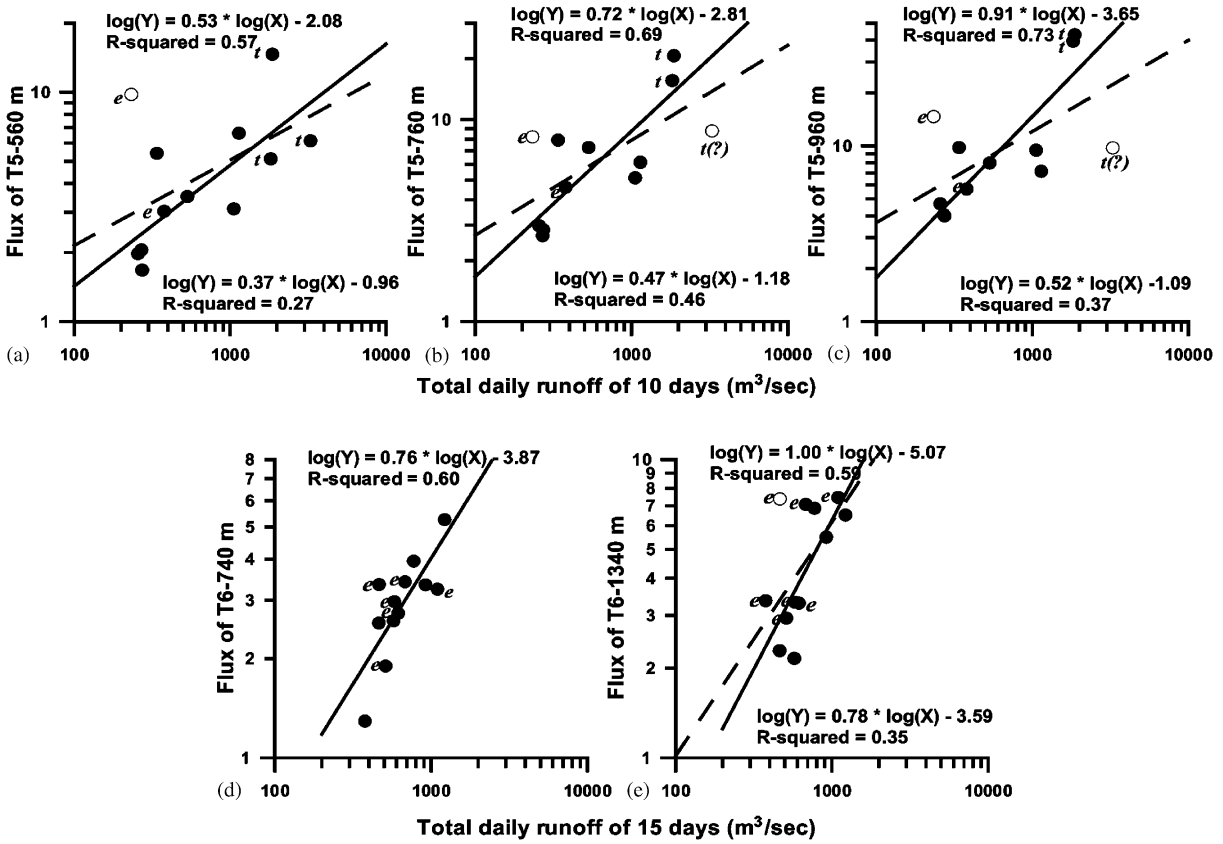

Fig. 8. Positive log–log relations between the observed sediment fluxes ($g/m^2/d$) for all traps and total daily runoff, integrating Lanyang Hsi mean daily runoff by selecting durations corresponding to the shifted periods for every cup. Dashed regression lines were drawn for all data points and their equations are shown in the lower part of plot; solid regression lines were constructed by excluding some anomalous data points (open circles) that cannot be simply interpreted by river sources, and their equations are listed in the upper part of the plot. Data points were marked with a "*t*" (typhoon) or an "*e*" (earthquake) if typhoons or large earthquakes ($M \geqslant 5.0$ R) took place during the collection periods of each cup. Most high flux data can be interpreted by either flood events or large earthquakes.

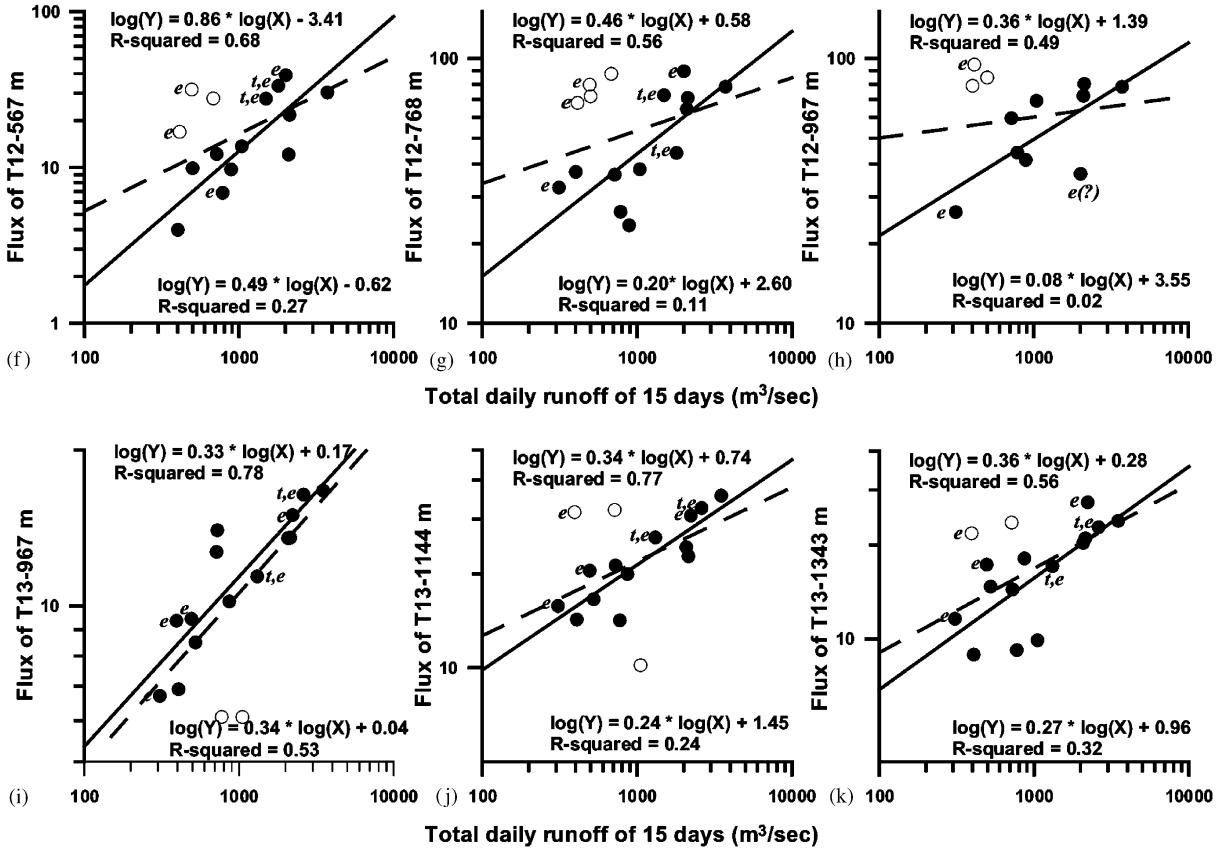

Fig. 8 (*continued*).

4.5. Enhancement of sediment fluxes by large earthquakes

In light of a few flux maxima (shown by open circles in Fig. 8) that could not be explained by the flood runoff alone, especially those observed on the northern slope of the Ilan shelf (T12), it was inferred that earthquakes might be either the direct or indirect cause because this area is in a tectonically active region. Also, two other facts were considered. First, the measured dates of the flux anomalies were usually in accord with the striking dates of some earthquakes of $M \geqslant 5.0$ R (or $M \geqslant 5.5$ R) with foci in the 24.50–25.50°N, 121–123°E (or 24–25.50°N, 121–124°E) quadrangle (Table 4) (http://www.iris.washington.edu). Second, because the slope north of the Ilan Shelf is rather steep ($> 3°$), the surface sediment on the slope readily becomes unstable and is then subject to resuspension or slumping once large earthquakes strike. For all individual flux data, the data points in Fig. 8 were labeled by an "*e*" if large earthquakes occurred in their measurement periods. For instance, an earthquake of $M = 6.9$ R striking on May 23, 1994 is presumed to be responsible for the third largest flux (cup 3, i.e. it would be the largest flux if the two fluxes of cups 11 and 12 driven by the typhoon flood are excluded) from the T5-960 m trap (Fig. 2). In particular, the two highest fluxes from the T12-960 m trap (95 g/m^2/d for cup 1) and the T12-768 m trap (80 g/m^2/d for cup 16) are quite abnormal because they corresponded to low runoff (Fig. 4). They apparently fall outside the

Table 4
Records of earthquakes larger than magnitude 5 (or 5.5) occurring in the 24.50–25.50°N, 121–123°E (or 24–25.50°N, 121–124°E) quadrangle during the collection periods of selected traps reported

Date (yymmdd)	Foci lat.(N), long. (E)	Magnitude	Trap samples
940523	24.10, 122.48	6.9	T5-cup 3 (o)[a]
940605	24.46, 121.86	6.9	T5-cup 4 (×)
940606	24.42, 121.19	5.1	T5-cup 4 (×)
940608	24.47, 121.75	7.9	T5-cup 4 (×)
940716	24.48, 121.78	6.8	T5-cup 4 (×)
941126	24.67, 122.24	5.5	T6-cup 2 (o)
941204	25.01, 122.77	5.0	T6-cup 2 (o)
941212	24.69, 122.54	5.0	T6-cup 3 (o)
941213	25.14, 122.86	5.6	T6-cup 3 (o)
950223	24.17, 121.68	6.5	T6-cup 7 (o)
950324	24.60, 121.93	5.6	T6-cup 9 (×)
950401	24.91, 122.11	5.3	T6-cup 10 (×)
950403	24.06, 122.30	6.1	T6-cup 10 (×)
950424	24.61, 121.73	5.3	T6-cup 11 (×)
960329	24.08, 122.20	5.8	T12/T13-cup 1 (o)
960609	24.92, 123.40	5.7	T12/T13-cup 8 (o)
960727	24.53, 122.05	5.0	T12/T13-cup 9 (o)
960729	24.49, 122.23	6.1	T12/T13-cup 9 (o)
960810	24.04, 122.67	5.7	T12/T13-cup 10 (o)
961126	24.08, 121.76	5.5	T12/T13-cup 14 (o)
961221	24.80, 122.82	5.3	T12/T13-cup 16 (o)

Note: Earthquake data were taken from http://www.iris.washington.edu.

[a] If the observed fluxes of the related trap samples are judged to be influenced by large earthquakes, they are labeled by circles; if not, by crosses. The time lag between earthquake and collection of affected sediment flux was taken into consideration when the judgments were made.

predicted relationships with the Lanyang Hsi runoff (Figs. 8g and h). Similarly, they seem to be caused by earthquakes of approximately $M \geqslant 5.0$ R (Table 4). Even though many flux data points deviating farther from regression lines could be explained by postulating a cause of earthquakes, not all earthquakes of $M \geqslant 5.0$ R induce elevated sediment fluxes. For example, the earthquake of $M = 6.9$ R striking on June 5, 1994 did not cause a pronounced increase in sediment fluxes observed at cup 4 of array T5. A variety of complicated parameters must be taken into account in the mechanisms of earthquake-driven sediment mass movements, such as frequencies and foci of large earthquakes. The measured impacts of earthquakes on sediment fluxes would also depend on deployment sites of trap arrays, i.e. the effect becomes weaker from the slope (i.e. T12 and T13) to the central trough (e.g. T6).

4.6. Uncertainties of the deep flows to sediment plumes

It is evident that the strength of the sediment plumes is controlled mainly by river runoff and occasionally by earthquakes. Besides, the deep flows should also be considered in driving the magnitudes of sediment fluxes. In this study, the hydrodynamic conditions were recorded by current meters attached to the trap mooring arrays. The hydrodynamic results recorded on both T5 and T6 trap arrays have been published elsewhere (Chung and Hung, 2000). Chung and Hung (2000), however, have not found any definite relations between the observed fluxes and the deep flows. The stick diagrams of low-frequency flow speeds and directions recorded at 951 and 1244 m of array T13 are displayed in Fig. 9. The flow at 951 m has changeable speeds of 1 to ~10 cm/s and a diverse N (including NE and NW) direction; whereas at 1244 m, it is characterized by an almost constant speed of less than 5 cm/s and a persistent direction of SE. The occasional high speeds and variable directions suggest that high-frequency flows (e.g. wave and tide) and the northward Kuroshio could sometimes appear at depths around 1000 m. Nevertheless, the influence of deep flows on the strength of suspended sediment plumes (or observed fluxes) seems not to be conclusive so far. On the other hand, it is similarly unclear whether the strong moving sediment plumes would drive deep flow, as found by Ogston et al. (2000). The only exception was that the elevated fluxes observed at cup 1 of both arrays T12 and T13 (Table 2) could likely be postulated to correlate with recorded high-speed flows (Fig. 9), even though they could also respond to a large earthquake, as mentioned above. In summary, the effects of the deep flows on the observed fluxes appear to be less significant compared to the flood runoff and large earthquakes.

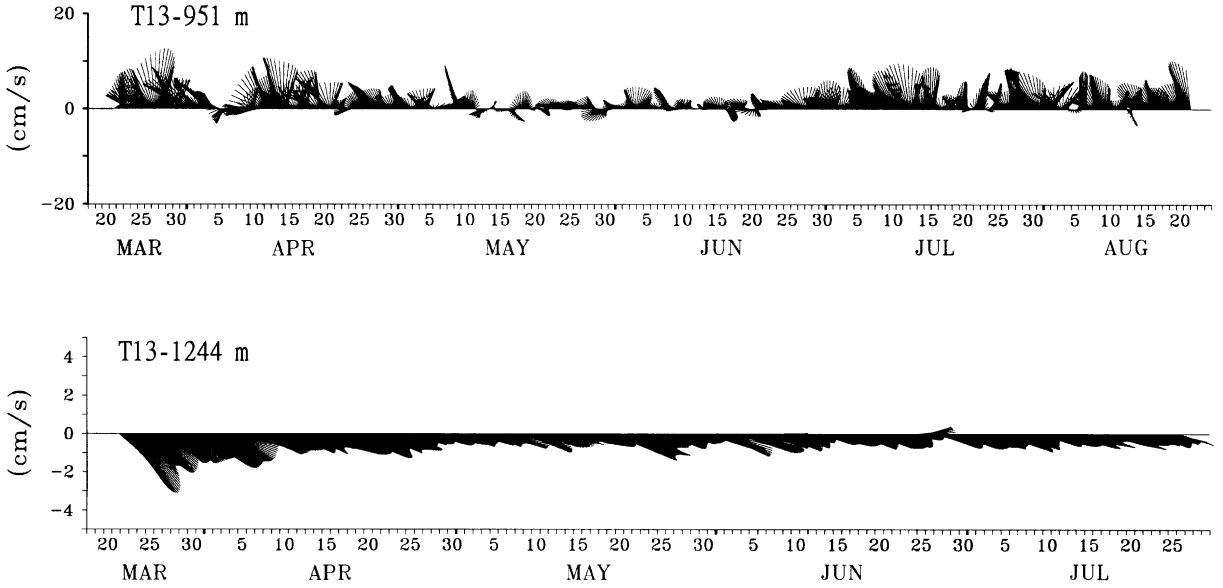

Fig. 9. Stick diagrams of flow speeds and directions recorded at 951 m (upper panel) and 1244 m (lower panel) from the first phase of the T13 deployment. Note that the two plots have different scales in both flow speed and time period. Results recorded at 1244 m in August were incomplete because of mechanical failure of the recorder.

4.7. A conceptual model illustrating sources and transport of the SOT sediments

A conceptual model is presented in Fig. 10 to briefly illustrate sources and transport of the SOT sediment. Also, it can explain what results of sediment fluxes were observed in the study and what forces drove these results. Terrigenous sediments from eastern Taiwan rivers (e.g. Lanyang Hsi) are delivered into the seas in rainy seasons; they may be transported quickly into the SOT during high runoff periods or remain temporarily on the Ilan Shelf and Ridge during low runoff periods. On the northern slope of the Ilan Shelf and Ridge, massive resuspension and slumping/sliding of the slope sediment, induced mainly by flood runoff (particularly during typhoon passages) and sometimes by large earthquakes, drive large-scale mass movements. These sediments would subsequently be transported downslope. The majority of reworked sediments are dispersed toward the central SOT in a matter of several days and the remainder of reworked sediments might be deposited on the lower slope. Together with various dynamical forces (e.g. steep topography, small submarine earthquakes, hydrodynamic disturbance, etc.), local resuspension could frequently take place along the slope–trough routes; this is based on the PAl spatial distribution. A scenario describing sediment transport of marginal sediments to deep basins in two steps, i.e. transport–deposition and resuspension–transport, has also been proposed by Heussner et al. (1999). The fluvial and reworked sediments that were originally deposited on the slope during flood events would be transported within discrete water layers and advected toward the trough; the upper, mid-depth and near-bottom nepheloid zones are perhaps developed in this way (Monaco et al., 1990; De Hass and Van Weering, 1997) and become the predominant supplier of the SOT sediments. The dense downslope sediment plumes would gradually go deeper with dispersal distance since they were generated on the northern slope of the Ilan Shelf and Ridge. With lateral transport the sediments would gradually fractionate their particle sizes and mineral assemblages and thus become diluted because of weakening of sediment

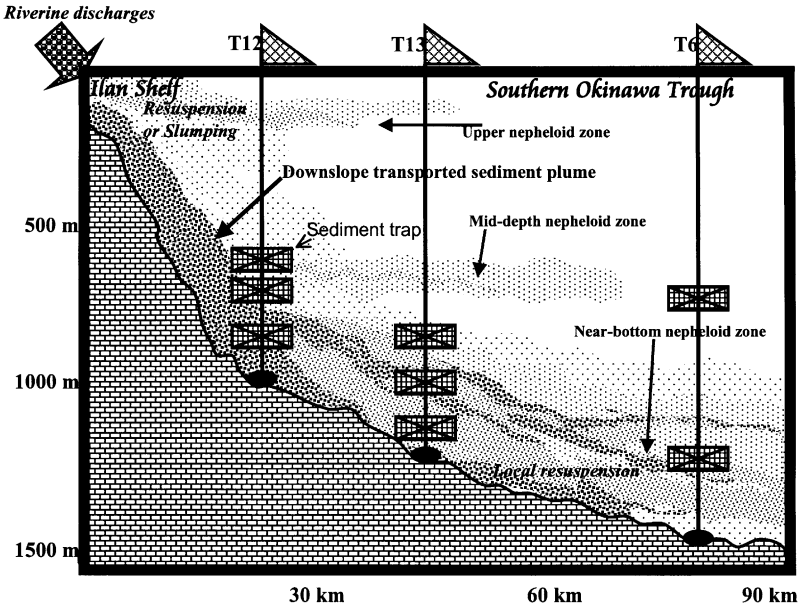

Fig. 10. A conceptual model describing a synoptic picture of the sources and transport of suspended and settling sediments along the vertical section from the Ilan Shelf/Ridge to the SOT. The SOT sediments may be supplied from the Lanyang Hsi (or eastern Taiwan rivers) primarily during typhoon passages or from the reworked slope sediments with a riverine origin caused by resuspension and slumping/sliding driven by earthquakes and topographic effects as well as hydrodynamic disturbances. The downslope and bottom transports are suggested to be the most important processes driving large-scale mass movements. Suspended particle plumes can develop at certain depths. The tongue-like, dotted areas indicate the suspended particle plumes that can form nepheloid layers; dot sizes and density represent particle size and the density of the plumes, respectively, illustrating that the particle size becomes smaller with transport distance and that the plume density becomes less with dispersal. The mid-depth nepheloid zone might explain why the observed sediment fluxes in the intermediate trap are higher than those in the upper and lower traps of array T13. Additionally, a small amount of bottom resuspension occurs locally on the transport route, particularly on the lower slope and trough seabed.

strength and addition of biogenic matter. This can explain why at station T12 the observed fluxes peaked at the deepest trap (967 m) and at station T13 at the intermediate trap (1144 m), and why the observed sediment fluxes decreased from traps T12 to T13, and from T13 to both T5 and T6.

5. Conclusions

A number of conclusions may be drawn from results of this study.

(1) The observed sediment fluxes in the SOT are much higher than in many other marginal seas. They exhibited synchronized variations at discrete depths for certain trap arrays. Spatial variability showed increasing trends with increasing depths and a decreasing tendency from the slope to the trough. Compositional results suggested the lithogenic (aluminosilicate) particles being the predominant components, accounting for at least 80%.

(2) The PAl spatial distribution showed a similar pattern to that of the observed fluxes, decreasing from the coastal to the offshore regions. Elevated PAl concentrations were found in the near-bottom water of the slope north to the Ilan Shelf and Ridge, which is a very unstable sedimentary environment. Three PAl plumes occurred at distinct depths and probably formed nepheloid layers that are an important source for the SOT terrigenous sediments.

(3) A positive relationship was found to exist between the observed fluxes and river runoff from eastern Taiwan (i.e. the Lanyang Hsi),

indicating that the magnitudes of particle fluxes are dependent on the contributions of river-borne particles, particularly during flood periods. It is elucidated how the flood sediments can be transported to the central trough so quickly. The contribution of episodic floods can account for at least 50% of the long-term (half a year) observed sediment fluxes in the SOT.

(4) A few flux extremes that cannot be explained by river runoff alone may be caused by large-scale mass movements induced by large earthquakes ($M \geqslant 5.0$ R). Our results demonstrated the observed fluxes dominated by episodic events.

(5) Coupling the data on sediment fluxes and PAl concentrations in the water column revealed that sediments from Taiwan rivers may be the most important source of the SOT sediments, as opposed to the sediments transported across the shelf, which are presumably from the Changjiang. Our conceptual model emphasizes that the down-slope transport of reworked sediments, driven by resuspension and slumping/sliding, was the major process dispersing the slope sediments to the trough.

Acknowledgements

We are grateful to three anonymous reviewers for their constructive comments. We thank the technicians and crew of R./V. *Ocean Researcher I* for their help with sampling. Thanks are also extended to Mr. K. Huang for pretreatment of samples and to Drs. S.J. Kao and W.T. Liang for their helpful comments. This research was financed by the National Science Council, ROC. SCH was supported through NSC grants (NSC 84-2611-M002A-007K2 and NSC 85-2611-M002A-026K2) to FJL.

References

Biscaye, P., Anderson, R.F., 1994. Fluxes of particulate matter on the slope of southern Middle Atlantic Bight: SEEP-II. Deep-Sea Research II 41, 459–509.

Boggs, S., Wang, W.C., Chen, J.C., 1979. Sediment properties and characteristics of the Taiwan shelf and slope. Acta Oceanographica Taiwanica 10, 10–49.

Chen, M.P., Lo, S.C., Lin, K.L., 1992. Composition and texture of surface sediment indicating the depositional environments off northeast Taiwan. Terrestrial, Atmospheric and Oceanic Sciences 3, 395–418.

Chen, S.K., 1995. Sediment accumulation rates and organic carbon deposition in the East China Sea continental margin sediments. M.S. Thesis, Institute of Oceanography, National Taiwan University, 80pp (in Chinese).

Chung, Y., Chang, W.C., 1995. Pb-210 fluxes and sedimentation rates on the lower continental slope between Taiwan and the South Okinawa Trough. Continental Shelf Research 15, 149–164.

Chung, Y., Chang, W.C., 1996. Uranium and thorium isotopes in marine sediments off northeastern Taiwan. Marine Geology 133, 89–102.

Chung, Y., Hung, K.W., 2000. Particulate fluxes and transport on the slope between the southern East China Sea and the South Okinawa Trough. Continental Shelf Research 20, 571–597.

De Hass, H., Van Weering, T.C.E., 1997. Recent sediment accumulation, organic carbon burial and transport in the northeastern North Sea. Marine Geology 136, 173–187.

Gardner, W.D., 1989. Baltimore Canyon as a modern conduit of sediment to the deep sea. Deep-Sea Research 36, 323–358.

Hasiotis, T., Papatheodorou, G., Bouckovalas, G., Corbau, C., Ferentinos, G., 2002. Earthquake-induced coastal sediment instabilities in the western Gulf of Corinth, Greece. Marine Geology 186, 319–335.

Heussner, S., Ratti, C., Carbonne, J., 1990. The PPS 3 time-series sediment trap and trap sample processing techniques used during the ECOMARGE experiment. Continental Shelf Research 10, 943–958.

Heussner, S., De Madron, X.D., Radakovitch, O., Beaufort, L., Biscaye, P.E., Carbonne, J., Delsaut, N., Etcheber, H., Monaco, A., 1999. Spatial and temporal patterns of downward particle fluxes on the continental slope of the Bay of Biscay (northeastern Atlantic). Deep-Sea Research II 46, 2101–2146.

Honjo, S., Spencer, D.W., Farrington, J.W., 1980. Deep advective transport of lithogenic particles in Panama Basin. Science 216, 516–518.

Honjo, S., Manganini, S.J., Poppe, L.J., 1982. Sedimentation of lithogenic particles in the deep ocean. Marine Geology 50, 199–220.

Hsu, S.C., 1998. Sources and transport of sediments and trace metal geochemistry in the water column off northeastern Taiwan. Ph.D. Thesis, Institute of Oceanography, National Taiwan University, 268pp (in Chinese with English abstract).

Hsu, S.C., Lin, F.J., Jeng, W.L., Tang, T.Y., 1998. The effect of a cyclonic eddy on the distribution of lithogenic particles in the southern East China Sea. Journal of Marine Research 56, 813–832.

Hsu, S.C., Lin, F.J., Jeng, W.L., Chung, Y., Shaw, L.M., 2003. Hydrothermal signatures in the southern Okinawa Trough detected by the sequential extraction of settling particles. Marine Chemistry 84, 49–66.

Ittekkot, V., Nair, R.R., Honjo, S., Ramaswamy, V., Bartsch, M., Manganini, S., Desai, B.N., 1991. Enhanced particle fluxes in Bay of Bengal induced by injection of fresh water. Nature 351, 385–387.

Kao, S.J., 1995. The biogeochemistry of carbon on an island of high denudation rate: a case study of the Lanyang Hsi watershed. Ph.D. Thesis, Institute of Oceanography, National Taiwan University, 262pp (in Chinese with English abstract).

Lee, C.S., Shor, G.G., Bibee Jr., L.D., Lu, R.S., 1980. Okinawa Trough: origin of a back-arc basin. Marine Geology 35, 219–241.

Lee, S.Y., 2001. Sedimentation dynamics off northeastern Taiwan elucidated from fallout nuclides. M.S. Thesis, Institute of Oceanography, National Taiwan University, 63pp (in Chinese with English abstract).

Letouzey, J., Kimura, M., 1986. The Okinawa Trough: genesis of a back-arc basin developing along a continental margin. Geophysics 125, 209–230.

Li, Y.H., 1976. Denudation of Taiwan island since the Pliocene epoch. Journal of Geology 4, 105–107.

Li, Y.H., 1994. Material exchange between the East China Sea and the Kuroshio Current. Terrestrial, Atmospheric and Oceanic Sciences 5, 625–631.

Lin, F.J., Chen, J.C., 1983. Textural and mineralogical studies of sediments from the southern Okinawa Trough. Acta Oceanographica Taiwanica 14, 26–41.

Lykousis, V., Roussakis, G., Alexandri, M., Pavlakis, P., Papoulia, I., 2002. Sliding and regional slope stability in active margin: North Aegean Trough (Mediterranean). Marine Geology 186, 281–298.

Lyne, V.D., Butman, B., Grant, W.D., 1990. Sediment movement along the US east coast continental shelf—II. Modelling suspended sediment concentration and transport rate during storms. Continental Shelf Research 10, 429–460.

Milliman, J.D., 1991. Flux and fate of fluvial sediment and water in coastal seas. In: Mantoura, R.F.C., Martin, J.M., Wollast, R. (Eds.), Ocean Margin Processes in Global Change. Wiley, Chichester, England, pp. 69–89.

Milliman, J.D., Meade, R.H., 1983. World-wide delivery of river sediment to the oceans. Journal of Geology 91, 1–21.

Milliman, J.D., Shen, H.T., Yang, Z.S., Robert, H.M., 1985. Transport and deposition of river sediments in the Changjiang estuary and adjacent continental shelf. Continental Shelf Research 4, 37–45.

Monaco, A., Biscaye, P., Soyer, J., Pocklington, R., Heussner, S., 1990. Particle fluxes and ecosystem response on a continental margin: the 1985–1988 Mediterranean ECOMARGE experiment. Continental Shelf Research 10, 809–839.

Mulder, T., Cochonat, P., 1996. Classification of offshore mass movements. Journal of Sedimentary Research 66, 43–57.

Narita, H., Harada, K., Tsunogai, S., 1990. Lateral transport of sediment particles in the Okinawa Trough determined by natural radionuclides. Geochemical Journal 24, 207–216.

Nair, R.R., Ittekkot, V., Manganini, S.J., Ramaswamy, V., Haake, B., Degens, E.T., Desai, B.N., Honjo, S., 1989. Increased particle flux to the deep ocean related to monsoons. Nature 338, 749–751.

Naudin, J.J., Gauwet, G.M., Chretiennot-Dinet, J., Deniaux, B., Devenon, J.L., Pauc, H., 1997. River discharge and wind influence upon particulate transfer at the land–ocean interaction: case study of the Rhone river plume. Estuarine, Coastal and Shelf Science 45, 303–316.

Nittrouer, C.A., 1999. STRATAFORM: overview of its design and synthesis of its results. Marine Geology 154, 3–12.

Ogston, A.S., Cacchione, D.A., Sternberg, R.W., Kineke, G.C., 2000. Observations of storm and river flood-driven sediment transport on the northern California continental shelf. Continental Shelf Research 20, 2141–2162.

Saito, C., Noriki, S., Tsunogai, S., 1992. Particulate flux of Al, a component of land origin, in the western North Pacific. Deep-Sea Research I 39, 1315–1327.

Sheu, D.D., Jou, W.C., Chung, Y.C., Tang, T.Y., Hung, J.J., 1999. Geochemical and carbon isotopic characterization of particles collected in sediment traps from the East China Sea continental slope and the Okinawa Trough northeast of Taiwan. Continental Shelf Research 19, 183–203.

Sibuet, J.C., Letouzey, J., Barbier, F., Charvel, J., Foucher, J.P., Hilde, T.W.C., Kimura, M., Chiao, L.Y., Marsset, B., Muller, C., Stephan, J.F., 1987. Back arc extension in the Okinawa Trough. Journal of Geophysical Research 92, 14041–14063.

Su, S.C., 2000. Sedimentation dynamics in the East China Sea: a multitracer approach. Ph.D. Thesis, Institute of Oceanography, National Taiwan University, 206pp (in Chinese with English abstract).

Tang, T.Y., Hsueh, Y., Yang, Y.J., Ma, J.C., 1999. Continental slope flow northeast of Taiwan. Journal of Physical Oceanography 29, 1353–1362.

Taylor, S.R., 1964. Abundance of chemical elements in the continental crust: a new table. Geochimica et Cosmochimica Acta 28, 1273–1285.

Water Resources Planning Commission, 1996. Hydrological Year Book of Taiwan, Republic of China, 1994. Ministry of Economic Affairs, Taipei, Taiwan, ROC, 393pp.

Water Resources Bureau, 1997a. Hydrological Year Book of Taiwan, Republic of China, 1995. Ministry of Economic Affairs, Taipei, Taiwan, ROC, 399pp.

Water Resources Bureau, 1997b. Hydrological Year Book of Taiwan, Republic of China, 1995. Ministry of Economic Affairs, Taipei, Taiwan, ROC, 400pp.

Wheatcroft, R.A., 2000. Oceanic flood sedimentation: a new perspective. Continental Shelf Research 20, 2059–2066.

Windom, H.L., Gross, T.F., 1989. Flux of particulate aluminum across the southern US continental shelf. Estuarine, Coastal and Shelf Science 28, 327–338.

Zhang, Y., Swift, D.J.P., Fan, S., Niedoroda, A.W., Reed, C.W., 1999. Two-dimensional numerical modeling of storm deposition on the northern California shelf. Marine Geology 154, 155–167.